HHS Public Access

Author manuscript

J Bone Miner Res. Author manuscript; available in PMC 2016 April 01.

Published in final edited form as:

J Bone Miner Res. 2015 April ; 30(4): 596–605. doi:10.1002/jbmr.2389.

Deletion of connexin43 in osteoblasts/osteocytes leads to impaired muscle formation in mice

Hua Shen, MD, PhD[1], **Susan Grimston, PhD**[2], **Roberto Civitelli, MD**[1,2], and **Stavros Thomopoulos, PhD**[1]

[1]Department of Orthopaedic Surgery, Washington University, St. Louis, MO, USA

[2]Division of Bone and Mineral Disease, Department of Internal Medicine, Washington University, St. Louis, MO, USA

Abstract

It is well-established that muscle forces are necessary for bone development as well as proper bone modeling and remodeling. Recent work has also suggested that bone acts as an endocrine organ that can influence the development of other organs. Connexin43 (Cx43), a gap junction protein that transduces mechanical signals, is an important determinant of cortical bone modeling. Using an osteoblast/osteocyte-specific ablation of the Cx43 gene (*Gja1*) driven by the 2.3 kb *Col1α1* promoter (cKO) in the mouse, this study confirmed reduced cortical bone thickness and density with expanded bone marrow cavity in the cKO humerus. Surprisingly, *Gja1* deletion in bone cells also affected skeletal muscle development, resulting in lower fast muscle weight, grip strength, and maximum absolute and specific tetanic forces (60–80%, 85%, and 50%, respectively, of WT mice). The normally fast twitch extensor digitorium longus (EDL) muscle exhibited increased slow twitch fibers in cKO mice. These muscle defects were accompanied by a 40–60% reduction in mRNA abundance for genes encoding osteocalcin in the humerus, relative to WT mice. Accordingly, both carboxylated and undercarboxylated isoforms of osteocalcin were reduced by over 30% in the circulation of cKO mice. Moreover, the active, undercarboxylated isoform of osteocalcin (glu-OC) promoted myotube formation in C2C12 myoblast cultures, and glu-OC injections to cKO mice rescued EDL muscle cross section area and grip strength *in vivo*. These findings demonstrate that Cx43 in osteoblasts/osteocytes indirectly modulates skeletal muscle growth and function, potentially via an endocrine effect of glu-OC.

Address correspondence to: Stavros Thomopoulos, PhD, Department of Orthopaedic Surgery, Washington University School of Medicine, 660 South Euclid Avenue, Campus Box 8233, St. Louis, MO 63110, USA. Phone: 314-362-8605. thomopouloss@wudosis.wustl.edu.

Author Contributions: HS, ST, and RC designed the study. HS performed the study, collected and analyzed data. HS, SG, RC, and ST interpreted data. HS and ST drafted the paper. HS, SG, RC, and ST critically revised and approved the final version of the manuscript and agreed to be accountable for all aspects of the work. HS and ST take responsibility for the integrity of the data analysis.

Additional Supporting Information may be found in the online version of this article.

Disclosures

Roberto Civitelli has a material transfer agreement with Zealand Pharma (Glostrup, Denmark) for the use of gap junction-modifying peptides but receives no honoraria or research funds from Zealand. He receives grant support from Amgen and Pfizer, and owns stock of Eli-Lilly, Merck, and Amgen. All other authors state they have no conflict of interest.

Keywords

connexin43; bone-muscle interactions; gap junction; osteocalcin

Introduction

Skeletal muscle contraction generates forces that are transmitted to bone and drive joint movement. Studies dating back to the 19th century have demonstrated a relationship between these forces and bone structure.[1] Specifically, developmental studies have showed that muscle contraction is necessary for bone morphogenesis and joint formation during early embryogenesis.[2,3] Furthermore, muscle forces drive postnatal accrual of bone mass and structural adaptation for optimal stress transfer and physical performance.[4–6] In the adult, muscle forces are essential for maintaining a balance between bone formation and bone resorption.[7,8] Recent studies have also suggested that muscle may influence bone growth by releasing osteogenic myokines such as IGF1 and FGF2.[9]

Connexin 43 (Cx43), a gap junction protein that is abundant in osteoblasts (OBs) and osteocytes (OCYs),[10] plays an important role in mechanotransduction. Gap junctions are intercellular channels that propagate nutrients and small signaling molecules among connecting cells to induce coordinated cellular responses.[11] Studies from several independent groups have shown that Cx43 in bone cells is involved in bone responsiveness to mechanical unloading [12,13] and loading.[14–16]

Biophysical and biochemical cues from muscle are clearly important for bone growth, but can bone similarly regulate muscle growth? It has been suggested that skeletal elements[17] and the chondrocytic paracrine factor Indian hedgehog[18] influence myogenesis during embryonic development. However, after birth, a densely packed mineralized extracellular matrix separates bone cells from skeletal muscle, so it is unlikely that soluble factors can diffuse from bone to muscle and regulate muscle growth through a paracrine mechanism. A more likely mechanism by which bone may regulate muscle growth is through hormones. Indeed, recent findings have demonstrated that bone might function as an endocrine organ regulating energy metabolism and reproduction[19,20], providing a putative mechanism of bone-muscle interaction that we pursued in the current study.

We hypothesized that deletion of the Cx43 gene, *Gja1*, from bone cells would: *i)* disrupt the transduction of the muscle-derived forces to bone and affect the subsequent development of bone and *ii)* disrupt the putative bone-to-muscle hormonal feedback and thereby compromise postnatal muscle formation and function. To test these hypotheses, we selectively deleted *Gja1* from OBs/OCYs to examine the role of OBs/OCY Cx43 in postnatal bone and muscle growth and a possible interaction between the two organs. Our results demonstrate the involvement of Cx43 in both bone and muscle formation and function and provide further evidence that bone is an endocrine organ that may regulate postnatal skeletal muscle growth.

Materials and Methods

Reagents

All reagents were purchased from Sigma-Aldrich (St. Louis, MO) unless otherwise specified.

Animals

All animal studies were conducted in accordance with the Public Health Service Policy on Humane Care and Use of Laboratory Animals and approved and overseen by the Animal Studies Committee at Washington University in St. Louis. Conditional knockout (cKO) mice depleted in *Gja1* in OBs/OCYs were generated as previously described.[21] In brief, the *Gja1* cKO mice were produced by crossing homozygous *Gja1*$^{flox/flox}$ mice with mice expressing Cre recombinase under the control of a 2.3 kb *α1(I) collagen* promoter fragment[22] and only one allele of *Gja1* (*Col1Cre;Gja1*$^{+/-}$). The resulting *Gja1* cKO mice (*Col1Cre;Gja1*$^{flox/-}$) and their WT equivalents (*Gja1*$^{flox/+}$) were studied at postnatal day 14, 28, and 56 (P14, P28, and P56). At least 16 WT and cKO animals per time point were allocated for initial phenotype characterization. An additional 15 P28 WT and cKO mice were allocated for further study on skeletal muscle. For osteocalcin (OC) injection experiments, 16 WT and 12 cKO mice were generated from 8 breeding pairs and received subcutaneous injections with either OC (60 ng/g, synthetic osteocalcin fragment 1-49, Sigma-Aldrich, O5761) or a corresponding volume of saline (6 μl/g) every other day from P5 to P28. The total sample size is summarized in Table 1. This sample size was chosen based on the expected variation and effect size calculated from previous studies.[12,23,24] The specificity of Cre expression was verified by crossing *Col1Cre* mice with either Ai14 (Jackson Labs)[25] or *mT/mG* (Jackson Labs)[26] Cre reporter mice. Based on a previous report, there were no expected differences in food intake between the WT and cKO mice.[23] No craniofacial abnormalities were found in the cKO mice.

Immunohistochemistry

Mouse shoulders with the supraspinatus (SS) muscles attached to the humeri were fixed in 4% paraformaldehyde (PFA; Electron Microscopy Sciences), decalcified, and sectioned to 5 μm in paraffin. After rehydration, antigen retrieval, and peroxidase inactivation, the sections were blocked and incubated with the following, with thorough washes after each step: rabbit anti-Cx43 antibodies (1:2000) at 37°C for 60 min, Anti-Rabbit IgG-Biotin antibodies (1:800) for 50 min, ExtrAvidin-Peroxidase (1:100) for 30 min, DAB-Plus Substrate (Life technologies) for 2 min, and Meyer's Hematoxylin Solution for 2 min.

Muscle cryosection and immunofluorescence staining

Freshly dissected extensor digitorium longus (EDL) muscles were orientated longitudinally, pinned on cork to keep their natural lengths (without visible stretching or curling), embedded in Tissue-Tek O.C.T, and snap frozen in melting isopentane. The frozen muscles were then transversely sectioned (7 μm) at the belly region at −20 °C. To determine muscle fiber isotype, the sections were blocked and incubated with the following at room temperature with thorough washes after each incubation: BA-F8 (Developmental Studies

Hybridoma Bank, DSHB; 1:50) or SC-71 (DSHB; 1:50) antibodies that recognize myosin heavy chain type I (MyHC I) or type IIa (MyHC IIa) fibers for 2 h, DyLight 488-conjugated donkey anti-mouse antibodies (Jackson ImmunoResearch; 1:400) for 1 h, 2 μg/ml Alexa Fluor 594-labeled wheat germ agglutinin (WGA; Molecular Probes) for 15 min. To examine Cx43 expression, after permeabilization and blocking, the sections were incubated with rabbit anti-Cx43 antibodies (1:400) at 4°C overnight, followed by Alexa 488-conjugated goat anti-rabbit antibodies (Invitrogen; 1:400) for 1 h and WGA staining for 15 min. Muscle fiber cross section area (CSA) was determined with an automated image analysis program CyteSeer 2.6.1 (Vala Sciences, Inc.).

Bone and muscle microCT

All samples were scanned with μCT40 (Scanco Medical AG, Switzerland) at 12 μm^3 voxel, 45 kVp, 177 μA, and 250 ms integration time except for the trabecular bone at P28 or younger, whose voxel resolution was 6 μm^3, and integration time was 200 ms. Entire SS muscles were scanned for total muscle volume and maximum CSA. EDL muscles were scanned for maximum CSA. For cortical bone properties, mouse humeri were scanned around the mid-diaphysis (1 mm in length) and analyzed for tissue mineral density (TMD), total CSA inside the periosteal envelope (Tt.Ar), cortical bone area (Ct.Ar), marrow area (Ma.Ar), cortical area fraction (Ct.Ar/Tt.Ar), and average cortical thickness (Ct.Th).[27] Humeral heads were scanned to determine trabecular bone properties. The metaphyses proximal to growth plates were analyzed for bone volume fraction (BV/TV), trabecular number (Tb.N), trabecular thickness (Tb.Th), and trabecular separation (Tb.Sp).[27]

Grip test

Forelimb grip tests were performed on P28 and P56 mice with grip wire attached to a digital force gauge (Chatillon DFE 2, San Diego Instruments). The mice were allowed to grip the pull bar on the grip wire with only their front paws and were steadily pulled back until they lost their grip with the lowest pull bar. Each mouse was given three trials and at least 5 min recovery time between trials. The peak tension during each trial was recorded with the attached force gauge. Mouse grip strength was presented as the average peak tension from the three trials.

Muscle force measurement

The isometric contractile force of the right gastrocnemius (GS) muscles from P28 mice was determined using a previously described method[24] and detailed in the supplemental data. Optimal muscle length (L_o) was first established using single 0.5 msec stimulation pulses at supramaximal stimulation voltages and then measured with a digital caliper. Maximum isometric tetanic force (P_o) was determined at L_o with a series of 0.5 msec stimulation pulses for a period of 450 msec at increasing frequencies (40 Hz–120 Hz). The tested muscles without their associated tendon and bone were then weighed on an analytical scale. The muscle fiber length (L_f) was calculated by multiplying L_o by 0.45.[28,29] Total fiber CSA was calculated by dividing muscle weight by muscle density (1.06 g/cm^3)[30] and L_f.[29] Specific P_o was calculated by dividing P_o by the total fiber CSA.

Quantitative realtime RT-PCR

Relative abundances of targeted gene expression in EDL, SS, GS, and soleus (SL) muscles and humeri were determined by SYBR-green based realtime RT-PCR as detailed previously.[31] All primers used for realtime RT-PCR were purchased from Qiagen.

Osteocalcin assay

All mice were fasted for 5–6 h prior to blood withdrawal. The plasma levels of carboxylated and under-carboxylated osteocalcin (OC) were determined using Mouse Gla-Osteocalcin and Glu-Osteocalcin High Sensitive EIA Kits (Takara Bio Inc), respectively.

C2C12 cell culture and immunostaining

C2C12 mouse skeletal myoblasts were kindly provided by Dr. Conrad Weihl at Washington University School of Medicine. The cells were maintained in growth medium containing 20% fetal bovine serum (Hyclone), 100 units/ml penicillin, and 100 μg/ml streptomycin (Pen/Strep; Gibco) in DMEM (Gibco) at less than 60% confluency. C2C12 differentiation was induced by replacing the growth medium with differentiation medium containing 2% horse serum (Hyclone) and Pen/Strep in DMEM at 90% confluency in the presence and absence of indicated dosages of OC (synthetic osteocalcin fragment 1-49, Sigma-Aldrich, O5761) for 72 h. The cultures were subsequently fixed, permeabilized, and stained with MF20 antibodies (DSHB; 1:10) that recognize sarcomere myosin, followed by DyLight 488-conjugated donkey anti-mouse antibodies (Jackson ImmunoResearch; 1:400) and Bisbenzimide H33258 (2 μg/ml). Digital images of two different areas were taken at 10 × magnification. Approximately 500 cells from each imaged area were quantified blindly for C2C12 fusion with Image J 1.47v software (National Institute of Health). The average percentage of C2C12 fusion was calculated as the ratio of the number of nuclei in multinucleated myotubes (containing at least three nuclei) and the number of total nuclei.

Statistical analysis

When data was normally distributed, two-tailed Student's t-tests were used to compare two groups and analyses of variance (ANOVA) followed by Tukey's posthoc tests (when appropriate) were performed to compare multiple groups. When data was not normally distributed, Mann-Whitney Rank Sum Tests were performed to compare two groups. Normally distributed data are shown as mean ± standard deviation bar plots and non-normally distributed data are shown as median and range (minimum and maximum, 1st and 3rd quartile) using box plots. All statistical analyses were performed using SigmaStat 3.5 (Systat Software, Inc.). Statistical significance was set at $p < 0.05$.

Results

Gja1 was selectively deleted in OBs/OCYs

To selectively delete *Gja1* in bone cells, a 2.3 kb *α1(I) collagen* promoter fragment was used to drive the expression of Cre recombinase in OBs and OCYs.[22] The specificity of Cre expression was verified by crossing the *Col1Cre* mice with Ai14 Cre reporter mice.[25] The resulting *Col1Cre;Ai14* mice revealed the expression of Col1Cre in bone but not

surrounding muscle tissues at P1.5 (Fig. 1A and 1B). This finding was corroborated via a second strain of *mTmG* Cre reporter mice.[26] Col1Cre expression was only seen in OBs and OCYs in humeral bone (Fig. 1C, 1E, and 1G) but not in the adjacent SS muscle (Fig. 1D, 1F, and 1H). No expression was seen in the SS tendon, its insertion into the humeral head, or the cartilage of the proximal humeral head of *Col1Cre;mTmG* mice at P14, P28, and P56 (Supplemental Fig. 1).

Using the Col1Cre/loxP recombination system, cKO mice with selective deletion of *Gja1* from OBs/OCYs were generated and validated using Cx43 immunostaining. Consistent with reports in the literature,[10] widespread Cx43 signals were detected in OBs and OCYs (including their processes) at the humeral diaphysis of WT P14 (Fig. 1I), P28 (Fig. 1K), and P56 (Fig. 1M) mice. Besides bone cells, Cx43 expression has also been reported in developing and regenerating muscle, but rarely in normal adult muscle.[32,33] Accordingly, localized Cx43 staining were detected at the boundaries of EDL muscle fibers in P28 WT mice (green; Fig. 1O). As expected, in the cKO mice, Cx43 expression was mostly absent in OBs and OCYs at the three postnatal ages investigated (Fig. 1J, 1L, and 1N) and remained unchanged in the skeletal muscle (Fig. 1P).

Cx43 deficiency in OBs/OCYs altered cortical bone architecture

Changes in humeral structure of *Gja1* cKO mice were examined in comparison to their WT littermates at P14, P28, and P56 by microCT analysis. Consistent with previous studies on adult mouse hindlimbs,[12] *Gja1* deletion in OBs/OCYs resulted in apparent defects in cortical bone structure in mice of all ages studied, including enlarged total and marrow area and reduced cortical bone thickness, density, and bone area fraction (Fig. 2A, B), but no detectable changes in cortical bone area (Fig. 2) and indexes for trabecular bone properties (Supplemental Tab. 1). These data confirmed that Cx43 function is involved in control of cortical bone modeling during postnatal bone growth.

Cx43 deficiency in OBs/OCYs led to reduced muscle mass and strength

Gja1 cKO mice were noticeably thinner but not shorter than their WT littermates. The average body weights of cKO mice were significantly lower than their WT counterparts, and this difference was more apparent in P28 ($p < 0.001$) and P56 ($p = 0.006$) mice than in P14 mice ($p = 0.619$; Fig. 3A). SS muscles were scanned to determine if the lower body weights of cKO mice were associated with lower muscle volumes. As showed in Fig. 3B, although the SS muscles from both WT and cKO mice grew significantly during the first 56 days in their life, the muscle volumes of cKO mice were significantly lower than those of WT mice. Consistent with the trends in body weights, the differences in muscle volumes between cKO mice and WT mice were larger at P28 ($p = 0.042$) and P56 ($p < 0.001$) than at P14 ($p = 0.851$). To determine whether the muscle abnormalities were muscle type specific, the wet weights of P28 GS, EDL, SL, and SS muscles were measured. All but the SL muscles showed lower weights in *Gja1* cKO mice compared to WT mice (Fig. 3C). Of note, EDL, SS, and GS muscles primarily consist of fast twitch fibers,[24,34,35] while the SL muscle contains a higher percentage of slow twitch fibers.[24,35] Thus, *Gja1* deletion in bone impairs muscle mass accrual during postnatal development, specifically for fast twitch muscles.

To determine if Cx43 deficiency in bone affected muscle function, forelimb grip tests and single muscle *ex vivo* force generation tests were performed. *Gja1* cKO mice possessed only 87% and 85% of grip strength of their WT counterparts at P28 and P56, respectively (Fig. 3D). Isometric force generated by isolated GS muscles was also lower in cKO mice. Specifically, the maximum absolute (Fig. 3E) and specific tetanic forces (Fig. 3F) of cKO muscle were both 50% of those of WT muscle. Therefore, Cx43 deficiency in bone affected both the mass and function of skeletal muscle during postnatal development.

Cx43 deficiency in OBs/OCYs altered muscle fiber quantity and composition

To determine how Cx43 bone deficiency affected skeletal muscle growth, the whole muscle CSA of SS muscles were compared between WT and cKO mice by microCT. In accordance with their muscle mass, *Gja1* cKO mice showed reduced maximum whole muscle CSA at P28 and P56 but not at P14 (Fig. 4A). Similarly, reduced maximum whole muscle CSA was detected in the EDL muscle of P28 cKO mice compared to that of WT mice (Fig. 4B). We further examined the muscle fiber CSA in P28 EDL muscle by immunofluorescence staining. Interestingly, despite the reduction in whole muscle CSA, no changes in average fiber as well as MyHC I- and MyHC IIa-specific fiber CSAs were detected (Fig. 4C). As muscle mass is directly related to muscle fiber numbers and CSA, these results indicated that cKO EDL muscles possessed fewer muscle fibers.

We next evaluated the relative abundance of *Mhy4* and *Mhy7* mRNA in P28 mouse muscles by quantitative realtime RT-PCR. *Mhy4* and *Mhy7* encode MyHC IIb and MyHC I proteins that compose the fast 2B and slow fibers, respectively.[35] Although *Gja1* deletion in OBs/OCYs did not affect *Mhy4* mRNA abundance in any of the muscles studied (Fig. 5A), the expression of *Mhy7* mRNA in EDL muscles from *Gja1* cKO mice was increased nearly threefold (Fig. 5B). Accordingly, an increased percentage of slow MyHC I fibers was detected by immunostaining in the cKO EDL muscle compared to the WT muscle (Fig. 5C and Supplemental Fig. 2). In addition, the percentage of fast MyHC IIa fibers tended to be higher in the cKO EDL muscle than in the corresponding WT muscle (Fig. 5C and Supplemental Fig. 2). Of note, both MyHC I and MyHC IIa fibers possess much lower contractile force and velocity than other fast fibers.[35] These results support the conclusion that deletion of *Gja1* from bone cells leads to an increase in slow twitch fibers in muscles that are normally made up of fast twitch fibers.

Cx43 deficiency in OBs/OCYs reduced circulating OC

We next considered possible endocrine mechanisms that could explain how bone specific deletion of *Gja1* can lead to changes in muscle development and growth. Among the soluble factors produced by bone cells, prostaglandin E2 (PGE2) may be released by OCYs via Cx43 hemichannels (i.e., half of a gap junction) after mechanical stimuli[36] and has been reported to facilitate myogenesis and muscle function.[20] However, prostaglandin E metabolites (PGEM) in the urine of *Gja1* cKO mice was nearly three-fold higher than in WT mice (Supplemental Fig. 3A); similarly, plasma PGEM was increased in cKO mice. Cox1 and Cox2 are enzymes required for the synthesis of prostaglandins. Surprisingly, no significant changes in *Cox1* and *Cox2* mRNA abundance were found in the humeri of cKO mice (Supplemental Fig. 3B). As PGE2 is produced by many different cell types, the higher

amount of systemic PGEM detected in the *Gja1* cKO mice may reflect a secondary effect of bone-specific *Gja1* deletion.

OC is an osteoblastic noncollagenous bone matrix protein. In mouse bone, OC is encoded by *bglap1* and *bglap2* genes.[37] While most OC is carboxylated on three glutamic acid residues (gla-OC), a small amount of OC is undercarboxylated (glu-OC).[19] This glu-OC is considered the active form of OC that can act as a multifunctional hormone in circulation.[19] *Gja1* cKO mice expressed 40–60% less *bglap1* and *bglap2* mRNA than their WT counterparts (Fig. 6A). Accordingly, reduced circulating glu-OC and gla-OC were detected in these cKO mice (Fig. 6B).

Cx43 deficiency in OBs/OCYs caused little change in insulin and energy homeostasis in fasting mice

Because OC enhances insulin secretion, sensitivity, and energy expenditure,[38] which are essential for normal muscle growth and function, we measured blood glucose and insulin levels in P28 and P56 mice after morning fast and found no significant differences between WT and cKO group (Supplemental Fig. 4A and 4B). Consistent with this, the mRNA abundance of *Insr*, *Irs1*, *Irs2*, and *Glut4* in SS muscle was not different between WT and cKO mice (Supplemental Fig. 4C); and mitochondrial oxidative capacity evaluated by mitochondrial volume density[39] in P28 EDL muscle was also comparable between WT and cKO mice (Supplemental Fig. 5). These results suggest that the muscle phenotypes seen in the *Gja1* cKO mice are not associated with disorders in insulin and energy metabolism, but further study is needed to confirm this.

glu-OC promoted myotube formation *in vitro* and rescued fast muscle CSA and grip strength of cKO mice *in vivo*

We then tested the effect of glu-OC on myoblast differentiation and myotube formation *in vitro* using the C2C12 myoblast cell line. A synthetic human OC consisting of amino acids 1-49 was used, representing the full mature sequence of unmodified glu-isoform OC. As shown in Fig. 6C–6H, glu-OC treatment led to a dose-dependent increase in myoblast fusion, an index of myotube formation, at doses of 10 to 100 ng/ml.

To establish a mechanistic link between the low circulating osteocalcin and muscle defects in cKO mice, we injected synthetic glu-OC subcutaneously in P5 mice, and measured body weight, EDL muscle CSA, and grip strength at P28. Although glu-OC injections did not lead to a full recovery of total body weight in cKO mice, the treatment did rescue EDL CSA and grip strength in cKO mice (Fig. 6I).

Discussion

Using the bone-specific *Gja1* cKO mice, this study explored bone-muscle crosstalk during postnatal development. We observed robust expression of Cx43 in OBs, OCYs, and OCY processes at P14, P28, and P56. Removal of Cx43 in OBs/OCYs resulted in cortical bone structural abnormalities consistent with accelerated endocortical bone resorption, as previously reported.[12,40,41] Results also revealed that Cx43 deficiency in OBs/OCYs during postnatal growth compromises skeletal muscle formation and function. Importantly,

we provide evidence that systemic OC stimulates muscle formation. These findings support the hypothesis that bone regulates muscle formation and reveal a novel role of OC in endocrine regulation of muscle growth.

Gja1 deletion in bone cells affects postnatal muscle growth and function, leading to ~30% and ~50% less than normal muscle mass and strength, respectively. The defect in muscle mass accrual was associated with lower number of muscle fibers, which may have resulted from either loss of existing muscle fibers (muscle degeneration) or from a defect in generating new muscle fibers (myogenesis). However, cKO muscles showed neither morphological signs of muscle degeneration (e.g., atrophy/reduction in muscle fiber CSA, centralized nuclei) nor apparent changes in mRNA abundances of genes that regulate myogenesis and muscle growth (Supplemental Fig. 6). The latter may be related to the time points studied, as muscle fiber numbers are determined before birth.[42,43] Accordingly, OB/OCY Cx43 deletion may have affected muscle fiber formation during embryonic development but not postnatally. This explanation may account for the lower body weight observed in mice with *Gja1* deletion driven by the *Col1* but not *bglap* promoter,[13] which targets fully differentiated OBs and OCYs.

Although muscle mass is often considered an indicator of muscle health, it is not necessarily correlated with muscle strength and performance.[20,44] Muscle fiber type, on the other hand, is closely related with muscle force and performance: fast twitch fibers generate greater force than slow twitch fibers.[35,44] OB/OCY *Gja1* deletion led to a reduction in muscle specific isometric force, and this reduction was accompanied by an increase in slow twitch fibers. These results are further corroborated by the findings that Cx43 deletion preferentially affected fast- but not slow-twitch muscle, and *Gja1* cKO mice exhibited weaker upper limb grip strength *in vivo* (an outcome that could be rescued by OC injection). Collectively, these findings strongly support a role of bone Cx43 in muscle formation and function.

Both *bglap1* and *bglap2* expression and circulating glu-OC were significantly reduced in *Gja1* cKO mice. These most likely reflect abnormalities in OB differentiation and function caused by OB/OCY Cx43 deficiency.[41,45] Indeed, previous results have demonstrated that *Runx2*, a transcription factor that controls OB differentiation and *bglap* expression,[46] is downregulated in Cx43-deficient OBs,[45] and the expression of other osteoblastic genes controlled by *Runx2* (e.g., *Col1alpha1* and *Opn*) is also downregulated in Cx43-deficient OBs.[45]

The reduction of *bglap* expression in bone and OC in circulation coupled with induction of myotube formation by glu-OC in C2C12 cells supports the notion that glu-OC influences postnatal muscle growth and function via an endocrine mechanism. This is further supported by the results from our *in vivo* rescue experiment, which showed that OC injection to postnatal cKO mice increased fast muscle CSA and rescued grip strength. Alternatively, glu-OC may regulate muscle growth and function via its roles in insulin secretion, sensitivity, and energy metabolism.[38] Based on this homeostatic mechanism, we would have predicted cKO mice to be hyperglycemic because of the lower circulating OC. However, we show that this is not the case; in fact, cKO mice showed normal glucose and insulin levels in the

fasting state. Thus, the muscle defects of *Gja1* cKO mice cannot be explained by disordered insulin and energy metabolism in the fasting state. However, we cannot exclude a role of energy metabolism on muscle function in conditions of increased glucose intake or energy expenditures in cKO mice.

A forward muscle-bone interaction model is proposed to describe the results of this study (Fig. 6J). In this model, muscle regulates bone modeling and function through mechanical stimulation and possible myokines. In return, bone influences muscle growth and function via the release of bone hormones such as glu-OC. Cx43 in bone cells is involved in elaboration of biophysical and biochemical signals from the muscle and for production of paracrine and endocrine signals. Removal of Cx43 from bone cells compromises bone-muscle cross talk. Others have demonstrated that signals from muscle affect bone homeostatic responses.[2–4,6,7,9] Here, we show that signals also flow in the opposite direction, from bone to muscle.

In summary, this study reveals that Cx43 is involved in bone-muscle cross talk and provides evidence for a novel role of OC in postnatal muscle formation and function. The later supports the notion that glu-OC could be a potential therapeutic approach to sarcopenia in elderly and frail patients.

Supplementary Material

Refer to Web version on PubMed Central for supplementary material.

Acknowledgments

The study was funded by the National Institutes of Health (R01 AR055580). Histologic sections were prepared by the Washington University Musculoskeletal Research Center (NIH P30 AR057235). The blood glucose assay was performed at the Washington University Diabetic Research Center (NIH P30 DK020579). Muscle sections for transmission electron microscopy were prepared by Dr. Wandy Beatty at Molecular Microbiology Imaging Facility at Washing University in St. Louis. The hybridomas BA-F8 and SC-71 were developed by Stefano Schiaffino, and MF 20 was developed by Donald A. Fischman. They were obtained from DSHB created by the NICHD of the NIH and maintained at The University of Iowa, Department of Biology, Iowa City, IA 52242.

Grant supporters: NIH R01 AR055580 to ST.

References

1. Wolff, J. The Law of Bone Remodeling. Maquet, P.; Furlong, R., translators. Berlin Heidelberg New York: Springer; 1986. (translation of the German 1892 edition)
2. Shwartz Y, Blitz E, Zelzer E. One load to rule them all: mechanical control of the musculoskeletal system in development and aging. Differentiation. 2013; 86:104–11. [PubMed: 23953954]
3. Rolfe R, Roddy K, Murphy P. Mechanical regulation of skeletal development. Curr Osteoporos Rep. 2013; 11:107–16. [PubMed: 23467901]
4. Ward KA, Caulton JM, Adams JE, Mughal MZ. Perspective: cerebral palsy as a model of bone development in the absence of postnatal mechanical factors. J Musculoskelet Neuronal Interact. 2006; 6:154–9. [PubMed: 16849825]
5. Pearl ML, Edgerton BW, Kon DS, Darakjian AB, Kosco AE, Kazimiroff PB, et al. Comparison of arthroscopic findings with magnetic resonance imaging and arthrography in children with glenohumeral deformities secondary to brachial plexus birth palsy. J Bone Joint Surg Am. 2003; 85-A:890–8. [PubMed: 12728041]

6. Schoenau E, Fricke O. Mechanical influences on bone development in children. Eur J Endocrinol. 2008; 159(Suppl 1):S27–31. [PubMed: 18787052]
7. Bloomfield SA. Disuse Osteopenia. Curr Osteoporos Rep. 2010; 8:91–7. [PubMed: 20425616]
8. Karinkanta S, Piirtola M, Sievänen H, Uusi-Rasi K, Kannus P. Physical therapy approaches to reduce fall and fracture risk among older adults. Nat Rev Endocrinol. 2010; 6:396–407. [PubMed: 20517287]
9. Hamrick MW, McNeil PL, Patterson SL. Role of muscle-derived growth factors in bone formation. J Musculoskelet Neuronal Interact. 2010; 10:64–70. [PubMed: 20190381]
10. Civitelli R. Cell-cell communication in the osteoblast/osteocyte lineage. Arch Biochem Biophys. 2008; 473:188–92. [PubMed: 18424255]
11. Goodenough DA, Paul DL. Gap junctions. Cold Spring Harb Perspect Biol. 2009; 1:a002576. [PubMed: 20066080]
12. Grimston SK, Goldberg DB, Watkins M, Brodt MD, Silva MJ, Civitelli R. Connexin43 deficiency reduces the sensitivity of cortical bone to the effects of muscle paralysis. J Bone Miner Res. 2011; 26:2151–60. [PubMed: 21590735]
13. Lloyd SA, Loiselle AE, Zhang Y, Donahue HJ. Connexin 43 deficiency desensitizes bone to the effects of mechanical unloading through modulation of both arms of bone remodeling. Bone. 2013; 57:76–83. [PubMed: 23891909]
14. Zhang Y, Paul EM, Sathyendra V, Davison A, Sharkey N, Bronson S, et al. Enhanced osteoclastic resorption and responsiveness to mechanical load in gap junction deficient bone. PLoS ONE. 2011; 6:e23516. [PubMed: 21897843]
15. Grimston SK, Watkins MP, Brodt MD, Silva MJ, Civitelli R. Enhanced periosteal and endocortical responses to axial tibial compression loading in conditional connexin43 deficient mice. PLoS One. 2012; 7:e44222. [PubMed: 22970183]
16. Bivi N, Pacheco-Costa R, Brun LR, Murphy TR, Farlow NR, Robling AG, et al. Absence of Cx43 selectively from osteocytes enhances responsiveness to mechanical force in mice. J Orthop Res. 2013; 31:1075–81. [PubMed: 23483620]
17. Lanser ME, Fallon JF. Development of wing-bud-derived muscles in normal and wingless chick embryos: a computer-assisted three-dimensional reconstruction study of muscle pattern formation in the absence of skeletal elements. Anat Rec. 1987; 217:61–78. [PubMed: 3454566]
18. Bren-Mattison Y, Hausburg M, Olwin BB. Growth of limb muscle is dependent on skeletal-derived Indian hedgehog. Dev Biol. 2011; 356:486–95. [PubMed: 21683695]
19. Karsenty G, Oury F. Biology without walls: the novel endocrinology of bone. Annu Rev Physiol. 2012; 74:87–105. [PubMed: 22077214]
20. Bonewald LF, Kiel DP, Clemens TL, Esser K, Orwoll ES, O'Keefe RJ, et al. Forum on bone and skeletal muscle interactions: summary of the proceedings of an ASBMR workshop. J Bone Miner Res. 2013; 28:1857–65. [PubMed: 23671010]
21. Castro CH, Stains JP, Sheikh S, Szejnfeld VL, Willecke K, Theis M, et al. Development of mice with osteoblast-specific connexin43 gene deletion. Cell Commun Adhes. 2003; 10(4–6):445–50. [PubMed: 14681055]
22. Dacquin R, Starbuck M, Schinke T, Karsenty G. Mouse alpha1(I)-collagen promoter is the best known promoter to drive efficient Cre recombinase expression in osteoblast. Dev Dyn. 2002; 224:245–51. [PubMed: 12112477]
23. Grimston SK, Brodt MD, Silva MJ, Civitelli R. Attenuated response to in vivo mechanical loading in mice with conditional osteoblast ablation of the connexin43 gene (Gja1). J Bone Miner Res. 2008; 23:879–86. [PubMed: 18282131]
24. Das R, Rich J, Kim HM, McAlinden A, Thomopoulos S. Effects of botulinum toxin-induced paralysis on postnatal development of the supraspinatus muscle. J Orthop Res. 2011; 29:281–8. [PubMed: 20803483]
25. Madisen L, Zwingman TA, Sunkin SM, Oh SW, Zariwala HA, Gu H, et al. A robust and high-throughput Cre reporting and characterization system for the whole mouse brain. Nat Neurosci. 2010; 13:133–40. [PubMed: 20023653]
26. Muzumdar MD, Tasic B, Miyamichi K, Li L, Luo L. A global double-fluorescent Cre reporter mouse. Genesis. 2007; 45:593–605. [PubMed: 17868096]

27. Bouxsein ML, Boyd SK, Christiansen BA, Guldberg RE, Jepsen KJ, Müller R. Guidelines for assessment of bone microstructure in rodents using micro-computed tomography. J Bone Miner Res. 2010; 25:1468–86. [PubMed: 20533309]
28. Burkholder TJ, Fingado B, Baron S, Lieber RL. Relationship between muscle fiber types and sizes and muscle architectural properties in the mouse hindlimb. J Morphol. 1994; 221:177–90. [PubMed: 7932768]
29. Larkin LM, Davis CS, Sims-Robinson C, Kostrominova TY, Van Remmen H, Richardson A, et al. Skeletal muscle weakness due to deficiency of CuZn-superoxide dismutase is associated with loss of functional innervation. Am J Physiol Regul Integr Comp Physiol. 2011; 301:R1400–7. [PubMed: 21900648]
30. Mendez J, Keys A. Density and composition of mammalian muscle. Metabolism. 1960; 9:184–8.
31. Shen H, Gelberman RH, Silva MJ, Sakiyama-Elbert SE, Thomopoulos S. BMP12 induces tenogenic differentiation of adipose-derived stromal cells. PLoS One. 2013; 8:e77613. [PubMed: 24155967]
32. Araya R, Eckardt D, Maxeiner S, Krüger O, Theis M, Willecke K, et al. Expression of connexins during differentiation and regeneration of skeletal muscle: functional relevance of connexin43. J Cell Sci. 2005; 118(Pt 1):27–37. [PubMed: 15601660]
33. Cea LA, Cisterna BA, Puebla C, Frank M, Figueroa XF, Cardozo C, et al. De novo expression of connexin hemichannels in denervated fast skeletal muscles leads to atrophy. Proc Natl Acad Sci U S A. 2013; 110:16229–34. [PubMed: 24043768]
34. Agbulut O, Noirez P, Beaumont F, Butler-Browne G. Myosin heavy chain isoforms in postnatal muscle development of mice. Biol Cell. 2003; 95:399–406. [PubMed: 14519557]
35. Schiaffino S, Reggiani C. Fiber types in mammalian skeletal muscles. Physiol Rev. 2011:1447–531. [PubMed: 22013216]
36. Cherian PP, Siller-Jackson AJ, Gu S, Wang X, Bonewald LF, Sprague E, et al. Mechanical strain opens connexin 43 hemichannels in osteocytes: a novel mechanism for the release of prostaglandin. Mol Biol Cell. 2005; 16:3100–6. [PubMed: 15843434]
37. Desbois C, Hogue DA, Karsenty G. The mouse osteocalcin gene cluster contains three genes with two separate spatial and temporal patterns of expression. J Biol Chem. 1994; 269:1183–90. [PubMed: 8288580]
38. Lee NK, Sowa H, Hinoi E, Ferron M, Ahn JD, Confavreux C, et al. Endocrine regulation of energy metabolism by the skeleton. Cell. 2007; 130:456–69. [PubMed: 17693256]
39. Schwerzmann K, Hoppeler H, Kayar SR, Weibel ER. Oxidative capacity of muscle and mitochondria: correlation of physiological, biochemical, and morphometric characteristics. Proc Natl Acad Sci U S A. 1989; 86:1583–7. [PubMed: 2922400]
40. Watkins MP, Norris JY, Grimston SK, Zhang X, Phipps RJ, Ebetino FH, et al. Bisphosphonates improve trabecular bone mass and normalize cortical thickness in ovariectomized, osteoblast connexin43 deficient mice. Bone. 2012; 51:787–94. [PubMed: 22750450]
41. Watkins M, Grimston SK, Norris JY, Guillotin B, Shaw A, Beniash E, et al. Osteoblast connexin43 modulates skeletal architecture by regulating both arms of bone remodeling. Mol Biol Cell. 2011; 22:1240–51. [PubMed: 21346198]
42. Shavlakadze T, Grounds M. Of bears, frogs, meat, mice and men: complexity of factors affecting skeletal muscle mass and fat. Bioessays. 2006; 28:994–1009. [PubMed: 16998828]
43. Rai M, Nongthomba U, Grounds MD. Skeletal muscle degeneration and regeneration in mice and flies. Curr Top Dev Biol. 2014; 108:247–81. [PubMed: 24512712]
44. Hoffman EP, Escolar D. Translating mighty mice into neuromuscular therapeutics: is bigger muscle better? Am J Pathol. 2006; 168:1775–8. [PubMed: 16723694]
45. Chung DJ, Castro CH, Watkins M, Stains JP, Chung MY, Szejnfeld VL, et al. Low peak bone mass and attenuated anabolic response to parathyroid hormone in mice with an osteoblast-specific deletion of connexin43. J Cell Sci. 2006; 119:4187–98. [PubMed: 16984976]
46. Ducy P, Zhang R, Geoffroy V, Ridall AL, Karsenty G. Osf2/Cbfa1: a transcriptional activator of osteoblast differentiation. Cell. 1997; 89:747–54. [PubMed: 9182762]

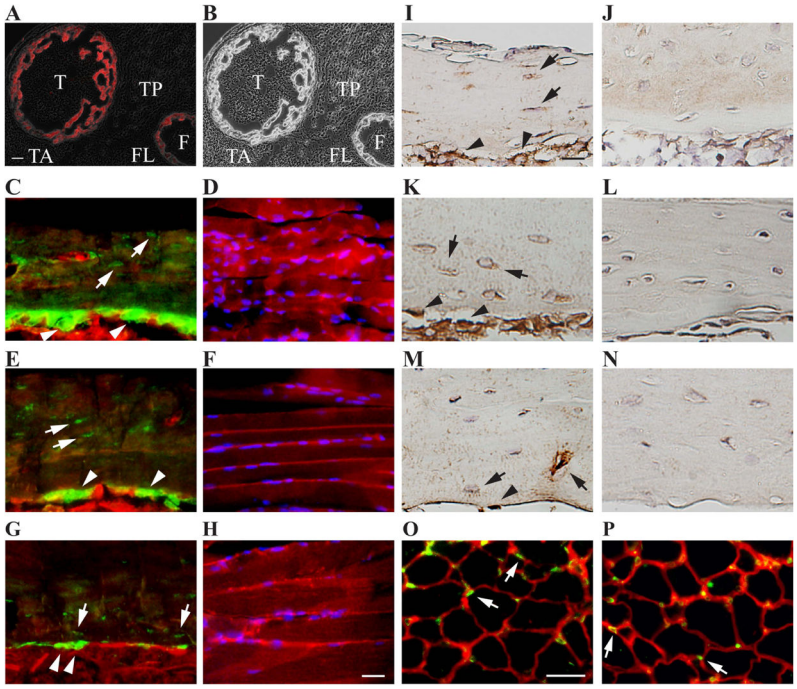

Fig. 1.

Selective deletion of Cx43 gene *Gja1* from OBs/OCYs. **A** and **B**, Representative fluorescence plus phase contrast (**A**) and phase contrast (**B**) images from lower hindlimb transverse section of P1.5 *Col1Cre;Ai14* mice. Col1Cre (in red) was detected in the tibia (T) and fibula (F) bones but not in the nearby tibia anterior (TA), tibia posterior (TP), and fibula longus (FL) muscles. Bar, 50 μm. N = 2. **C** – **H**, Representative fluorescence images of humeral diaphysis (**C, E, G**) and SS muscle (**D, F, H**) from coronal sections of P14 (**C** and **D**), P28 (**E** and **F**), and P56 (**G** and **H**) *Col1Cre;mTmG* mouse shoulders. Col1Cre (in green) was detected in OCYs (white arrows) and OBs (white arrow heads) but not in SS muscles counterstained with DAPI (in blue). N = 3 at each time point. Bar, 100 μm. **I** – **N**, Representative images of Cx43 immunohistochemistry staining (in dark brown) on the coronal sections of humeral diaphysis of WT (**I, K, M**) and *Gja1* cKO (**J, L, N**) mice at P14 (**I** and **J**), P28 (**K** and **L**), and P56 (**M** and **N**). Bar, 50 μm. N = 3 for each condition. **O** and **P**, Representative immunofluorescence staining for Cx43 expression (in green) on the transverse sections of P28 EDL muscle from WT (**O**) and *Gja1* cKO (**P**) mice. Cx43 positive signals (white arrows) were detected at the junctions of neighboring muscle fibers (labeled in red with WGA) in both WT and cKO muscles. Bar, 25 μm. N = 3 and 4 for O and P, respectively.

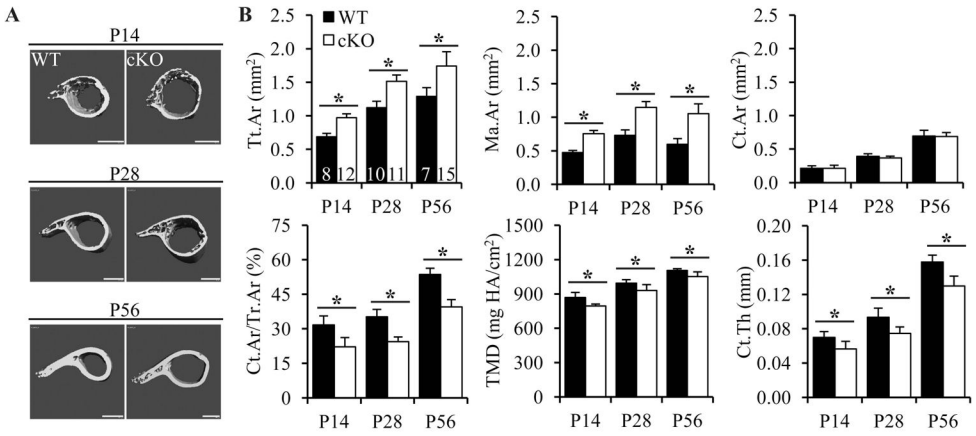

Fig. 2.

Cx43 deficiency in OBs/OCYs altered cortical bone microarchitecture. **A** and **B,** Representative 3D microCT images (**A)** and analyses of cortical bone indexes (**B**) at the mid-diaphysis of WT and *Gja1* cKO humeri. Bars, 500 μm in A. $p < 0.001$ for both genotype and age for all indexes, except for Ct.Ar, where $p = 0.493$ for genotype, 2-way ANOVA followed by Tukey's test. The sample sizes for A and B are indicated in the first plot of B. *, $p < 0.05$.

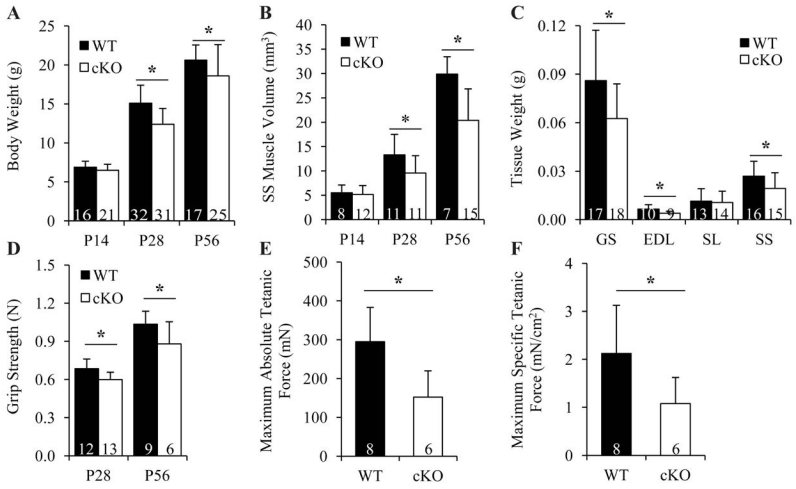

Fig. 3.

Cx43 deficiency in OBs/OCYs led to defects in muscle mass and strength accrual. **A,** Changes in mouse body weights. $p < 0.001$ for both genotype and age, 2-way ANOVA followed by Tukey's test. **B,** Changes in SS muscle volumes. $p < 0.001$ for both genotype and age, 2-way ANOVA followed by Tukey's test. **C,** Comparison of wet muscle weights between P28 WT and cKO mice. $p = 0.014$, 0.026, 0.777, and 0.039 for GS, EDL, SL, and SS muscle, t-test. **D,** Changes in mouse forelimb grip strength. $p < 0.001$ for both genotype and age, 2-way ANOVA followed by Tukey's test. **E** and **F,** Comparison of maximum absolute **(E)** and specific **(F)** tetanic forces of GS muscles between P28 WT and *Gja1* cKO mice. $p = 0.012$ and 0.040 for E and F, respectively, t-test. Sample sizes are indicated at the bottom of each column plot. *, $p < 0.05$.

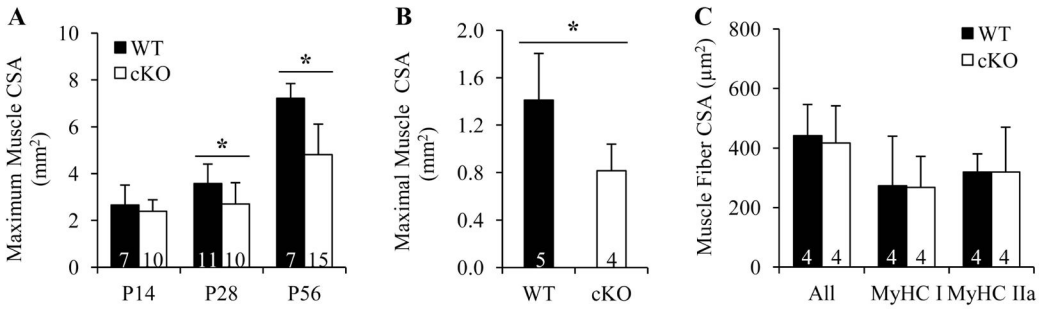

Fig. 4.

Cx43 deficiency in OBs/OCYs reduced muscle but not muscle fiber CSA. **A** and **B,** Maximum whole muscle CSA of SS (**A**) and EDL (**B**) muscle determined by microCT. p = 0.563, 0.048, and <0.001 at P14, P28, and P56 in A, 2-way ANOVA followed by Tukey's test; p = 0.032 in B, t-test. **C,** Average CSAs of all, MyHC I, and MyHC IIa fibers evaluated by immunofluorescence staining. p = 0.772, 0.963, and 0.999, respectively, t-test. Sample sizes are indicated at the bottom of each column. *, $p < 0.05$.

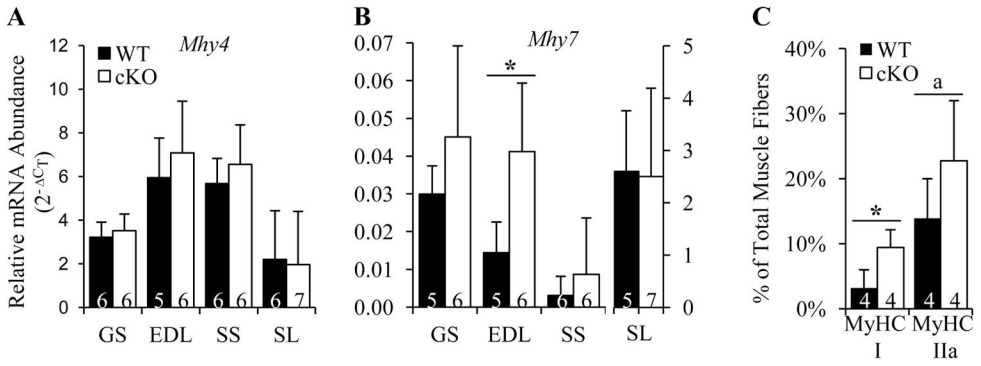

Fig. 5.

Cx43 deficiency in OBs/OCYs altered muscle fiber composition. **A** and **B**, Changes in mRNA expression of *Mhy4* (**A**) and *Mhy7* (**B**) in P28 mouse skeletal muscles. $p = 0.496$, 0.406, 0.335, and 0.857 for GS, EDL, SS, and SL muscle, respectively in A; $p = 0.655$, 0.014, 0.411, and 0.911 for GS, EDL, SS, and SL muscle, respectively in B, t-test. **C,** Changes in the composition of MyHC I and MyHC IIa fibers in P28 EDL muscles. *, $p = 0.019$, a, $p = 0.161$, t-test. Sample sizes are indicated at the bottom of each column.

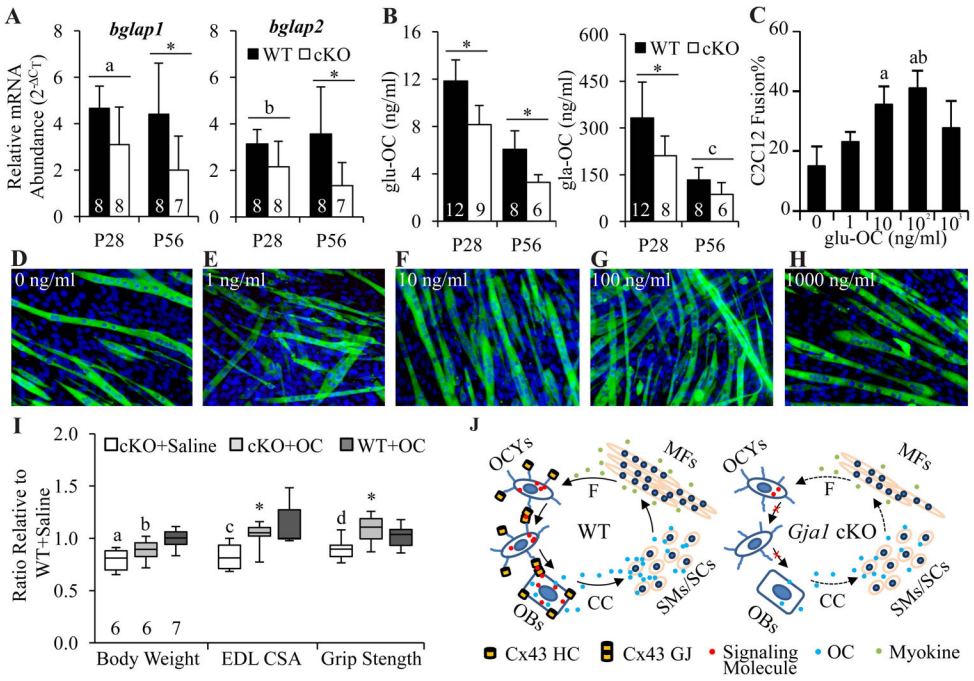

Fig. 6.

Bone *Gja1* deletion led to a decrease in osteoblastic osteocalcin, which is also myogenic. **A**, Relative abundance of *bglap1* and *bglap2* mRNA in humeri of WT and *Gja1* cKO mice. *bglap1*, $p = 0.002$ and 0.264 for genotype and age; *bglap2*, $p = 0.002$ and 0.688 for genotype and age; a, $p = 0.065$, b, $p = 0.144$, *, $p < 0.05$, two-way ANOVA followed by Tukey's test. **B,** Changes in plasma glu-OC and gla-OC in WT and *Gja1* cKO mice. glu-OC, $p < 0.001$ for both genotype and age; gla-OC, $p = 0.006$ and <0.001 for genotype and age; c, $p = 0.292$, *, $p < 0.05$, 2-way ANOVA followed by Tukey's test. Sample sizes for A and B are indicated at the bottom of each column plot. **C–H,** Representative fluorescence images (**D–H**) and quantifications (**C**) for the effects of glu-OC on C2C12 myoblast differentiation. C2C12 differentiation was induced in the presence of 0 (**D**), 1 (**E**), 10 (**F**), 100 (**G**), and 1000 (**H**) ng/ml of glu-OC for 72 h. The culture was stained with MF20 antibody and Bisbenzimide H33258 for sarcomere myosin (in green) and nuclei (in blue), respectively. Bar, 50 μm. Three independent experiments were performed for each treatment. $p = 0.005$ for glu-OC concentration; a, $p < 0.05$ compared to 0; b, $p < 0.05$ compared to 1; one-way ANOVA followed by Tukey's test. **I,** Changes in body weight, maximum EDL muscle CSA, and grip strength in P28 mice after subcutaneous injection of glu-OC. a, b, c, and d, $p = 0.002$, 0.040, 0.007, and 0.036, respectively, compared to WT+saline, Mann-Whitney rank sum test; *, $p = 0.032$ compared to cKO+saline, t-test. Sample size for each group is indicated at the bottom of the first three boxes from the left. **J,** Model for Cx43-mediated bone-muscle interaction. CC, circulation; F, muscle force; GJ, gap junction; HC, hemichannel; MF, muscle fiber; SC, satellite cell; SM, skeletal myoblast.

Table 1

Summary of animal numbers.

N	P14	P28	P56
WT	16	48	17
cKO	21	43	25